A Study on the Nonuniform Deformation of PTFE Membrane During its Tentering Transverse Stretching

Yu-Hai Guo, Jian-Yong Chen, Jing-Xin Gao, Hua-Peng Zhang, Xin-Xing Feng

Key lab of Advanced textile materials and manufacturing technology, Ministry of Education, Materials and Textiles College, Zhejiang Sci-tech University, Zhejiang 310018, Hangzhou, People's Republic of China

Received 25 September 2008; accepted 16 October 2009
DOI 10.1002/app.31605
Published online 17 December 2009 in Wiley InterScience (www.interscience.wiley.com).

ABSTRACT: To understand the deformation of biaxially stretched polytetrafluoroethylene (PTFE) membrane during the tenter frame transverse stretching process, a finite element analysis (FEA) model was established to study the stress and displacement distribution during the transverse stretching. The morphology, pore size, and mechanical properties of the membrane were also characterized. It has been found from the experimental and FEA simulation results that the tentering transverse stretching of PTFE membrane is a nonuniform stretching, the stress and displacement distribution of the PTFE membrane during tentering is nonuniform because of the nonuniform deformation and the ease of yield and plastic deformation originated from the specific structure of the virgin PTFE particles. The nonuniform thickness and pore size distribution across the membrane width resulted from this nonuniform deformation was also characterized and discussed.
 J Appl Polym Sci 116: 1124–1130, 2010

Key words: polytetrafluoroethylene (PTFE); membranes; biaxiality; tentering transverse stretching; nonuniform deformation

INTRODUCTION

Microporous polytetrafluoroethylene (PTFE) membrane and its composite membranes have been applied into many fields as functional garments, medical care products, filtering and separation, and electronics[1–5] because of their unique microporous structure and excellent chemical inertness. One widely employed method for producing porous polytetrafluoroethylene (PTFE) membranes is by a series of mechanical operations including paste extrusion, rolling, and biaxial stretching under different temperatures and then heat treatment.[6–8] In recent years, some papers have been published concerning the preparation, structure-property relationship, and morphological dependence on the stretching conditions of porous PTFE membranes. Hatzikiriakos extensively investigated the processing conditions including extrusion die design, resin molecular structure, and lubricant concentration on the preforming behavior and properties of PTFE paste extrudates, and a model was developed to study the effects of die design on the preforming process.[9–11]

Kurumada et al. studied the morphological parameters, the process of structure generation and their dependence on the stretching parameters (stretching rate, stretching ratio, stretching sequence) of porous PTFE membrane.[12] Kitamura et al. further studied the relationship between the porous morphological parameters and the stretching parameters, and then discussed the formation mechanism of porous structure in PTFE membranes based on the distinctive microstructures of the PTFE particles.[13,14] Kitamura investigated the morphology change and properties improvement on heat treatment above 320°C.[15] Chen studied the structural dependence of PTFE porous membrane on the stretching conditions.[16]

But the porous PTFE membranes of the aforementioned studies were prepared by a two-step sequential equal-stretching process, which is far different from the industrial tentering biaxial stretching process. Transverse tenter stretching after first longitudinal stretching is widely adopted in industry because of its ease of process control and large scale of productivity. PTFE membrane undergoes complicated heat and mechanical coupled deformation

Correspondence to: H.-P. Zhang (roc.zhp@163.com).
Contract grant sponsor: Research and Development Program of China(863); contract grant number: 2007AA06Z310.
Contract grant sponsor: Natural Science Foundation of Zhejiang; contract grant number: Y407269.
Contract grant sponsor: Science Foundation of Zhejiang, Sci-Tech University (ZSTU); contract grant number: 0601290.
Contract grant sponsor: Program for Changjiang Scholars and Innovative Research Team in University; contract grant number: IRT0654.
Contract grant sponsor: Hi-Tech.
Contract grant sponsor: National Science Foundation of China; contract grant number: 20806074.

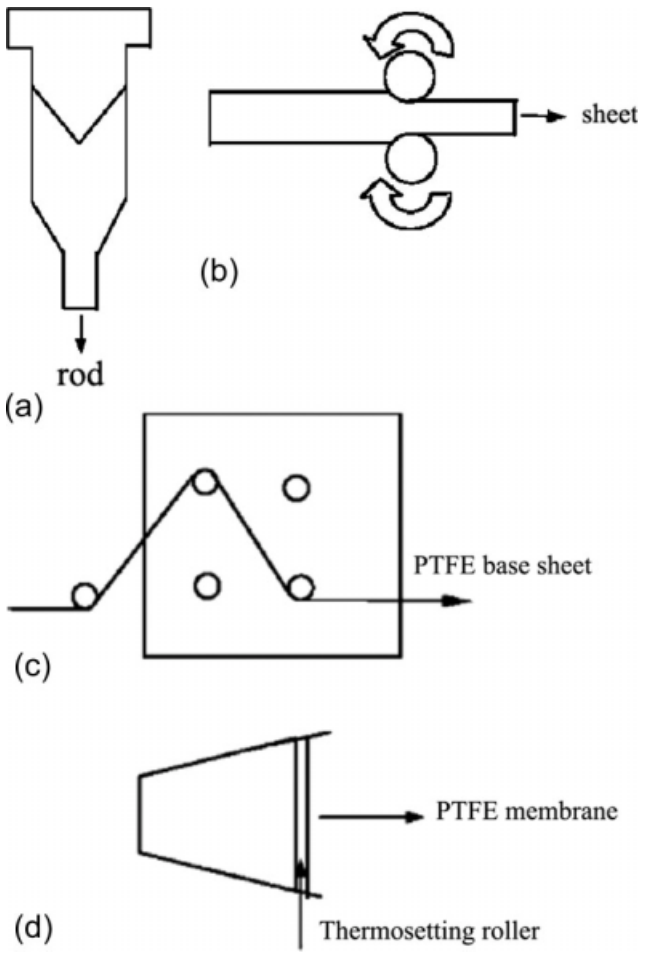

Figure 1 Process of PTFE membrane. (a) extrusion (b) rolling (c) longitudinal stretching in oven (d) transverse stretching and setting.

during its stretching, especially during the tenter transverse stretching process, which is a nonuniform or unequal stretching in itself. Owing to the higher research costs and complicated deformation, the tenter stretching process was always studied by trial-and-error experiments in the industrial controlling of the so-called "black box" transverse stretching process.[17]

Although many results on structural and properties nonuniformity induced by the tentering process of biaxially oriented films such as BOPP, BOPET have been published and well documented, few reports have been reported concerning the nonuniformity of porous PTFE membranes prepared by tentering biaxial stretching. In this article, a finite element analysis (FEA) model for the tentering process of PTFE membrane was established to analyze the nonuniform distribution of the stress and strain in the tenter stretching zone, and the thickness and pore size nonuniformity of the PTFE membrane was also characterized and discussed in this article.

EXPERIMENTAL

PTFE membrane preparation

Expanded PTFE fine powder produced by emulsion polymerization (3.0×10^6 in number averaged molecular weight, F-103, Daikin Industries) was mixed with naphtha as a lubricant (20%) and then aged for about 24 h at 37°C. It was first pre-extruded into a cylindrical billet with diameter of about 100 mm, and then ram extruded into a rod of about 13 mm in diameter. Thereafter, the rod was rolled between two metal rollers into a sheet. The rolled sheet was longitudinally stretched by rollers in an oven at 210°C, whereas the naphtha was being evaporated to produce the PTFE base sheet with a thickness of 120 μm in this study. The stretching ratio was varied from 100% to 400%. Then the PTFE base sheet underwent a transverse stretching with a tenter frame machine at 140–170°C. The two opposite sides of the PTFE base sheet was clipped by a running chain, which held the base sheet tightly and stepwise stretched the base sheet into the final width of the PTFE membrane. Finally, the PTFE membrane was heat set at 320°C for about 5s on a stainless steel roller. The process is schematically shown in Figure 1.

PTFE membrane characterization

SEM observation

The membrane morphology was examined using an Amary-1845FE scanning electron microscope (SEM) after the membrane samples were gold sputtering coated.

Pore size measurement

Pore sizes of the membranes characterized by mean flow pore sizes (M.F.P.) were obtained through

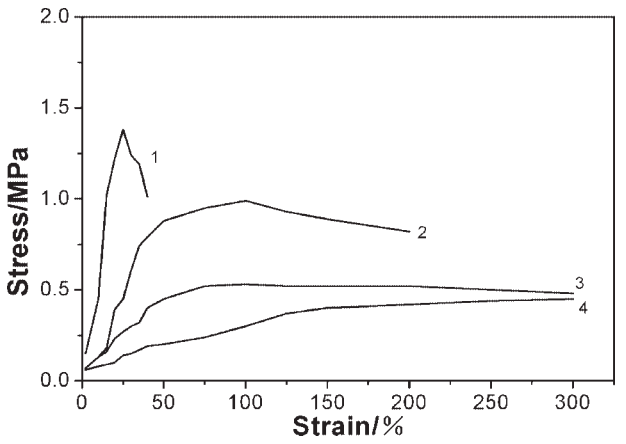

Figure 2 Stress–strain curves of the PTFE base sheet at stretching temperature of (a) 35°C, (b) 90°C, (c) 140°C, (d) 170°C.

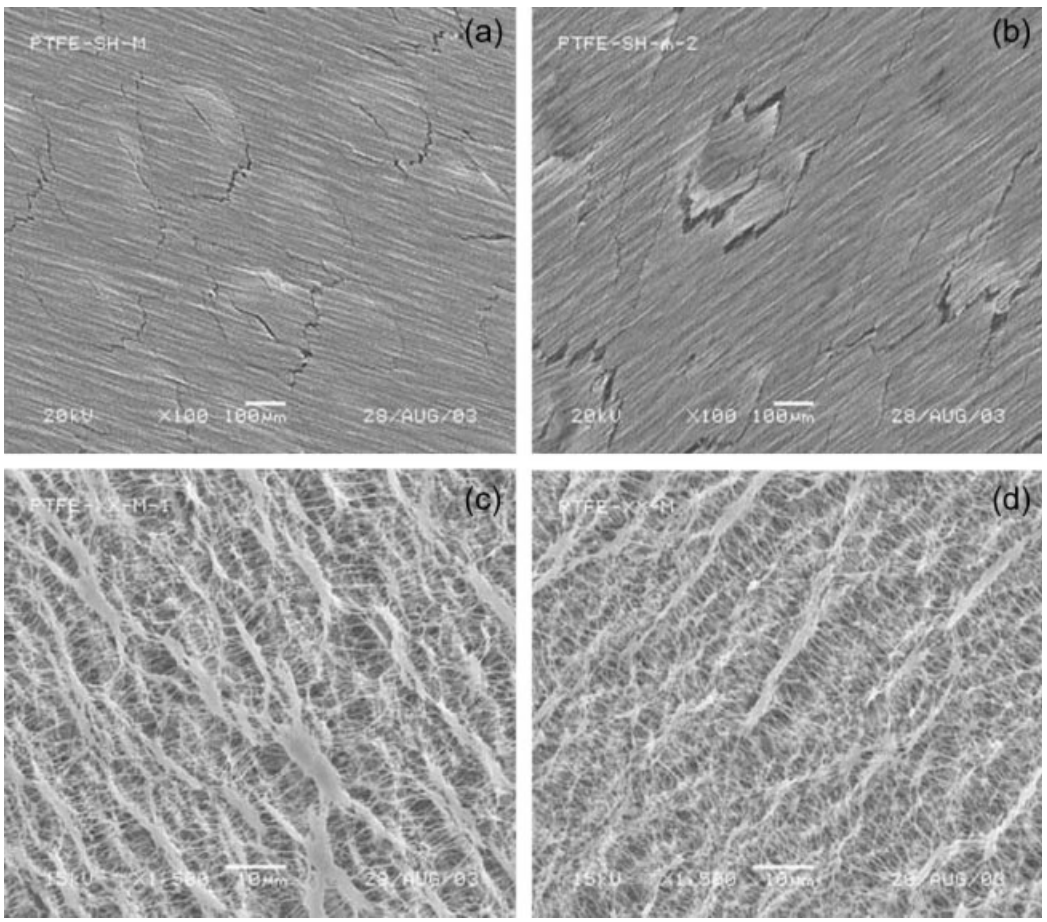

Figure 3 SEM of the PTFE membrane with different stretching temperature of (a) 35°C, (b) 90°C, (c) 140°C, (d) 170°C.

Coulter Porometer II manufactured by Coulter Electronics. Testing principle and theory of the Coulter Porometer II is a modified bubble point technique, which has been described in detail in references.[18,19]

Mechanical properties test

Mechanical properties of the PTFE base sheet between 35–170°C after longitudinal stretching was measured through an INSTRON 5565 tensile testing apparatus. The PTFE sheet was first cut into size of 150 mm (length) × 25 mm (width), and the gauge length of the mechanical tester was 10 mm, and the rate of the crosshead was set at 300 mm/min.

RESULTS AND DISCUSSION

Transverse stretching behavior of the PTFE base sheet

The typical stress–strain curves of PTFE base sheet under different transverse stretching temperatures is given in Figure 2, from which it can be found that the PTFE base sheet changes from brittle to ductile characteristic with the raise of stretching temperature, suggesting the temperature sensitivity of PTFE base sheet on stretching temperatures. The membrane can be stretched into a porous structure with less nodes and fibrils under temperature as low as 35°C, but it breaks at stretching strain of 25% [Figs. 2(a), 3(a)]. Even at 90°C, the PTFE base sheet still undergoes breakage at strain of 100% (Figure 2b and Figure 3b), but with the temperature increasing above 140°C, the PTFE base sheet can be stretched even more than 300% without a breakage (Figure 2c and Figure 3c). It was found that in order to achieve small nodes and more fibrils, the transverse stretching temperature must be higher than the α transition

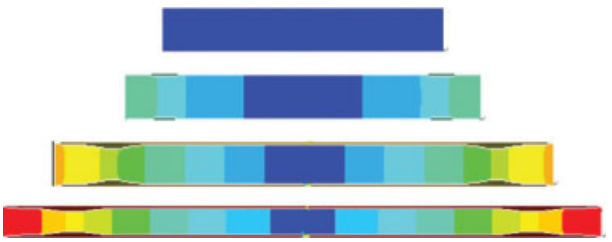

Figure 4 Simulated displacement distributions of equally transverse stretched PTFE base sheet. [Color figure can be viewed in the online issue, which is available at www.interscience.wiley.com.]

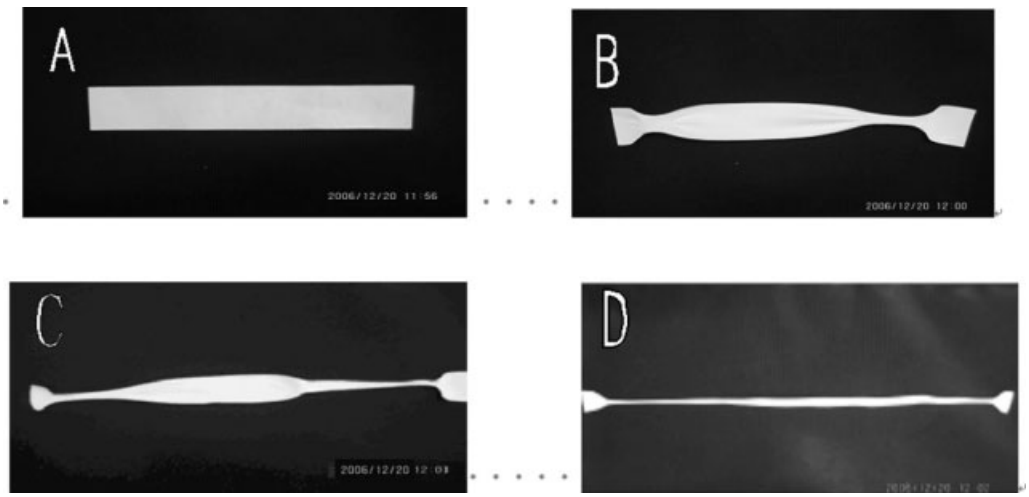

Figure 5 Observations of equally transverse stretched PTFE base sheet under 170°C.

temperature (at about 120–140°C) of PTFE,[20] which is attributed to the molecular motions in the crystalline phase and the restricted amorphous phase. To get more fibrils and small nodes, after the PTFE base sheet has been yielded during stretching, there must be a plastic stress plateau, i.e. a steady tensile stress,[13] which corresponds to the steady fibrils forming process. In this article, the transverse stretching temperature was chosen at 170°C, which would ensure a steady tensile stress after it yielded.

FEA on the transverse stretching process of PTFE membrane

To understand the stress distribution field during the transverse stretching process, a finite element model was established to analyze the stress and strain filed in the PTFE membrane. In this model, following assumptions were assumed: (1) the temperature field was uniform and constant across the PTFE base sheet, (2) the PTFE base sheet was mechanically isotropic, (3) the effect of viscocity was omitted, that is, the rate or viscous effect was omitted during the elastic and plastic deformation process. Because the PTFE base sheet would undergo large deformation and plasticity, a 2D 8-node structural solid element (Plane82) with plane stress has been adopted; this element formulation has plasticity, creep, swelling, stress stiffening, large deflection, and large strain capabilities. A nonlinear inelastic rate independent isotropic hardening plastic material model with Mises multilinear plasticity was selected based on the model assumptions. To simulate the deformation process, a series of step wise displacement loads were imposed on the boundary of the two edges of the PTFE base sheet.

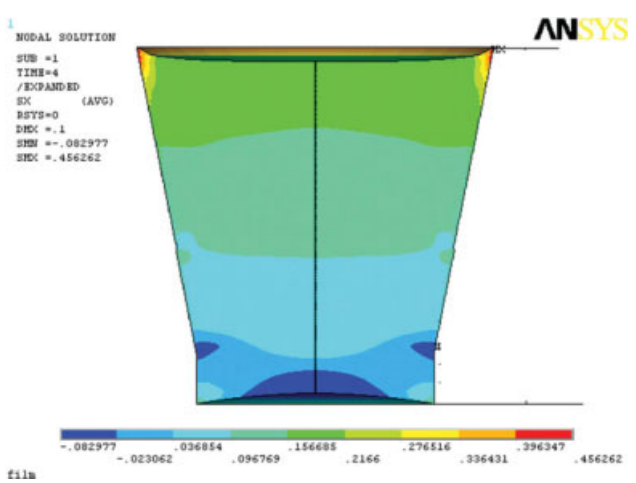

Figure 6 Transverse stress (σ_x) distribution. [Color figure can be viewed in the online issue, which is available at www.interscience.wiley.com.]

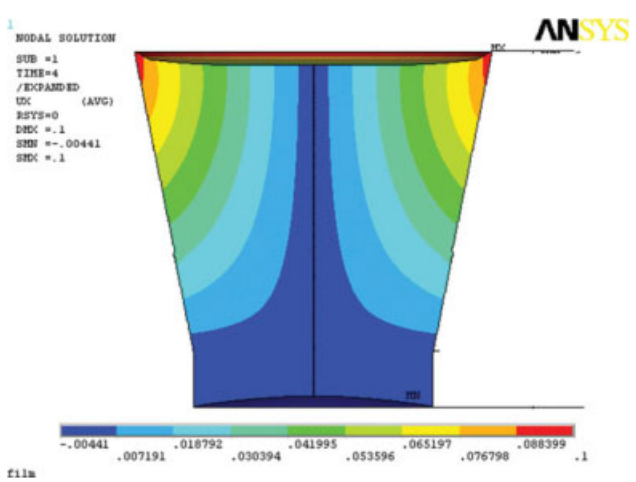

Figure 7 Transverse displacement (u_x) distribution. [Color figure can be viewed in the online issue, which is available at www.interscience.wiley.com.]

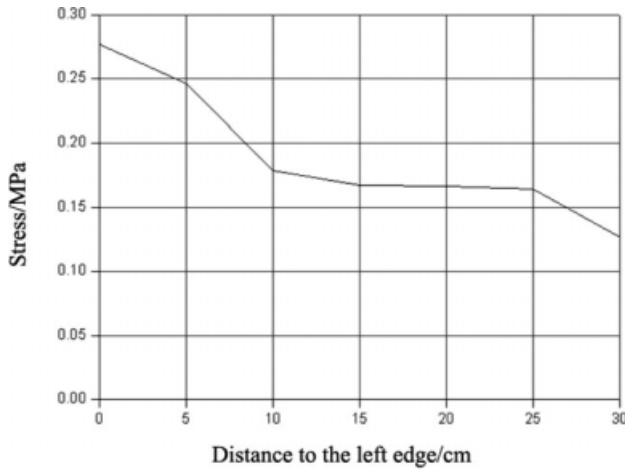

Figure 8 Transverse stress (σ_x) distribution.

FEA simulation on the equally transverse stretching of PTFE base sheet

To check the feasibility of finite element simulation, first equally transverse stretching of PTFE base sheet was experimentally conducted, and the FEA simulation was carried out on the above assumptions. Because transverse stretching was conducted under 170°C, the mechanical properties of the PTFE base sheet under 170°C was used, which was illustrated in the stress–strain curve of Figure 2(d). The elastic modulus and poisson's ratio was measured as 3.0 MPa and 0.2, respectively.

The simulation model size of the PTFE base sheet was 40 mm long, 10 mm wide, and 120 μm thick. The simulated displacement contour of the PTFE base sheet after it was stretched by a total of displacement of 10 mm, 30 mm, and 40 mm, respectively was given in Figure 4, and the experimental results were shown in Figure 5, where stretching ratios of the samples increase from A to D, and the stretching rate is 300 mm/s. From Figures 4 and 5, it

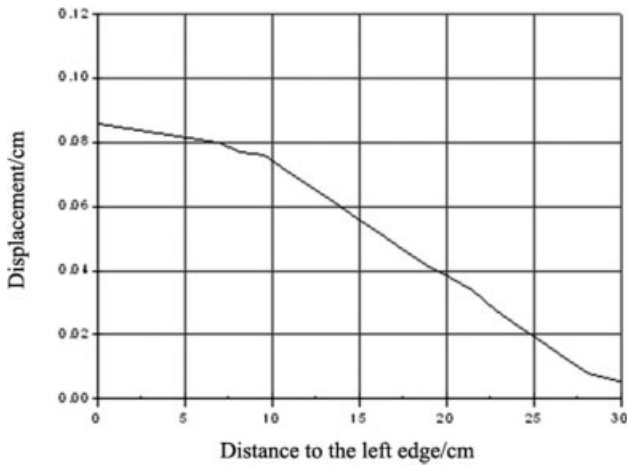

Figure 9 Transverse displacement (u_x) distritbution.

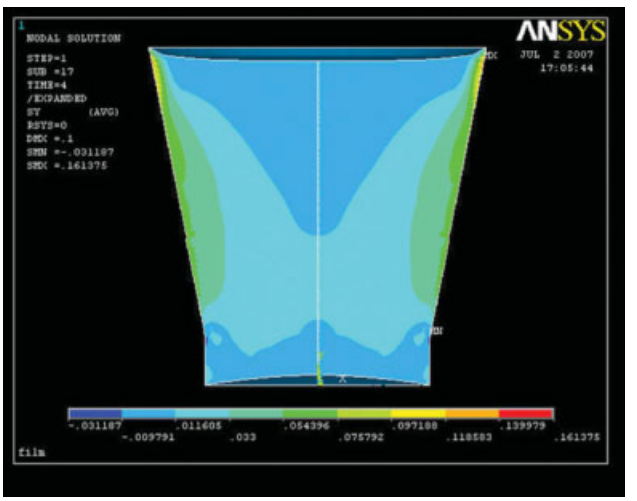

Figure 10 Longitudinal stress (σ_y) distribution. [Color figure can be viewed in the online issue, which is available at www.interscience.wiley.com.]

was seen that the PTFE base sheet was deformed gradually from the middle to the two edges, with the two edges had larger displacement and strain; moreover, the PTFE base sheet exhibited obvious necking phenomena, indicating that even under equal stretching, the deformation of the PTFE base sheet was nonuniform at different stretching stages. The deformational similarity between the deformed experimental and simulated results also suggested the feasibility of the FEA model in the stress and strain distribution analysis.

FEA simulation on the tenter frame transverse stretching of PTFE base sheet

A finite element model with initial PTFE base sheet, 60 cm long, 40 cm wide, and 120 μm thick, was

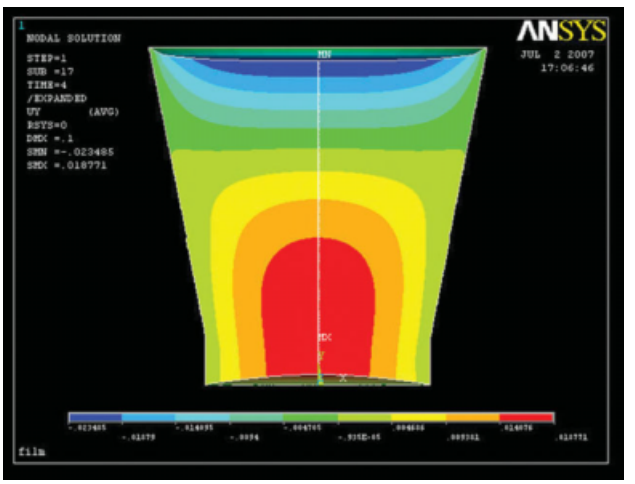

Figure 11 Longitudinal displacement (u_y) distribution. [Color figure can be viewed in the online issue, which is available at www.interscience.wiley.com.]

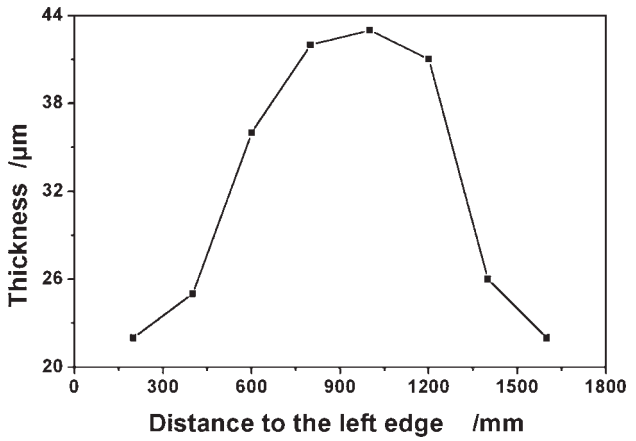

Figure 12 Membrane thickness vs distance to the left edge.

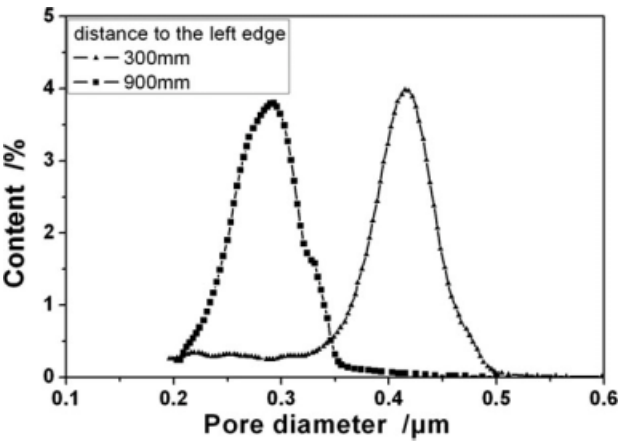

Figure 13 Micropore structure of PTFE membrane vs. distance to the left edge.

established. Based on the transverse symmetry of the model, only half of the solid model was employed during computation.

Transverse stress and displacement distribution during tenter frame stretching

The simulated transverse stress and displacement distribution of PTFE membrane after tenter frame stretching were shown in Figures 6 and 7 respectively. From Figures 6 and 7, it can be seen that with gradual enlargement of the width of PTFE base sheet, the transverse stress and displacement along the longitudinal direction are gradually increasing; and the transverse stress and displacement exhibit an ascending trend from the middle to the two edges of the PTFE membrane along the transverse direction. Figures 8 and 9 gives the transverse stress and displacement along the transverse at a distance of 55 cm from the entrance of the PTFE base sheet, respectively.

Longitudinal stress and displacement distribution during tenter frame stretching

Figures 10 and 11 gives the simulated results of longitudinal stress and displacement distribution of PTFE base sheet during the tenter frame stretching, respectively. Due to the longitudinal contraction from transverse stretching and inelastic properties of the PTFE base sheet, there are a nonuniform longitudinal stress and displacement during transverse stretching of the PTFE base sheet. From Figure 11, it is obviously observed that in the middle of the membrane, the longitudinal displacement is larger than the two edges at the same distance from the entrance of the PTFE base sheet.

The effects of transverse stretching on the thickness and pore size of PTFE membrane

A PTFE base sheet 250 mm wide and 120 μm thick was transversely stretched into a final width of 1800 mm membrane with a stretching rate of 80 mm/s at stretching temperature of 170°C. The thickness of the membrane was measured at different locations of the membrane; the results were given in Figure 12, from which it can be seen that the membrane was thicker in the middle but thinner in the two edges. Easy slippage between crystalline ribbons in the PTFE fine particles and easy cleavage inside the ribbons, and low stress activation energy to fibril formation facilitate the stretching process of PTFE base sheet into a mircoporous membrane. But when the PTFE base sheet was stretched, the stress and displacement was transferred from the two edges to the middle of the PTFE membrane, which can be seen in Figures 8 and 9. Therefore, the lateral area of the membrane is more stretched than the middle zone when the base sheet is stretched to the width of 1800 mm, leading to a thicker middle area across the width of the PTFE membrane.

TABLE I
Effect of Transverse Stretching on the Micropore Sizes of PTFE Membrane

Distance to the left edge (mm)	100	300	600	900	1200	1500	1700
Micropore diameter (μm)	0.513	0.423	0.346	0.281	0.361	0.418	0.528

Pore sizes of the membrane after transversely tenter frame stretching were given in Figure 13 and Table I, from which it can be seen that the central area of the membrane has a smaller pore size, the lateral zone of the membrane has a larger pore size. Moreover, the pore size of the membrane is related to the thickness of the membrane, the thicker area has a smaller pore size, which means the thicker central area is less stretched than the lateral thinner area.

CONCLUSIONS

Transverse stretching through tentering process in manufacturing of two-step biaxially stretched PTFE microporous is a nonuniform stretching, which will lead to nonuniform deformation of the membrane. Due to the easy yield and plastic deformation of the PTFE base sheet, which results from the special folded ribbon-like crystalline structure of the emulsion-polymerized virgin PTFE particles, the PTFE base sheet is inclined to nonuniform deformation, even in the equal transverse stretching. A preliminary FEA model was established to analyze the stress and displacement distribution of the PTFE membrane during tentering transverse stretching. Experimental and simulated results indicate that the central area of the membrane has lower stress and displacement than the bilateral area, which results in the larger thickness and lower pore size in the central area.

References

1. Hao, X. M.; Zhang, J. C. Membr Sci Technol (Chese) 2005, 25, 2.
2. Hao, X. M. Doctoral Thesis, Donghua University, 2004.
3. Hao, X. M.; Zhang, J. C.; Guo, Y. H. International Symposium on Advanced Materials and Their Related Science, Beijing University of Chemical Technology, 2003.
4. Guo, Y. H.; Chen, J. Y.; Hao, X. M.; Zhang, J. C.; Feng, X. X.; Zhang, H. P. J Mater Sci 2007, 42, 2081.
5. Huang, J. Z.; Zhang, J. C.; Hao, X. M.; Guo, Y. H. Euro Polym J 2004, 40, 667.
6. Yamazaki, E. U.S. Pat. 4,110,392 (1978).
7. Gore, R. W. U.S. Pat. 3,953,566 (1976).
8. Gore, R. W. U.S. Pat. 3,962,153 (1976).
9. Ariawan, A. B.; Ebnesajjad, S.; Hatzikiriakos, S. G. Powder Technol 2001, 121, 249.
10. Ariawan, A. B.; Ebnesajjad, S.; Hatzikiriakos, S. G. Polym Eng Sci 2002, 42, 1247.
11. Ariawan, A. B.; Ebnesajjad, S.; Hatzikiriakos, S. G. Can J Chem Eng 2002, 80, 1153.
12. Kurumada, K. I.; Kitamura, T.; Fukumoto, N.; Oshima, M.; Tanigaki, M.; Kanazawa, S. J Membr Sci 1998, 149, 51.
13. Kitamura, T.; Kurumada, K. I.; Tanigaki, M.; Ohshima, M.; Kanazawa, S. I. Polym Eng Sci 1999, 39, 2256.
14. Rahl, F. J.; Evanco, M. A.; Fredericks, R. J.; Reimschuessel, A. C. J Polym Sci 1972, 2, 1337.
15. Kitamura, T.; Okabe, S.; Tanigaki, M.; Kurumada, K. I.; Ohshima, M.; Kanazawa, S. I. Polym Eng Sci 2000, 40, 809.
16. Chen, S. Chese J Chem Phy (Chese) 2005, 18, 228.
17. Kanai, T.; Campbell, G. A. In Film Processing; Hanser: Munich, 1999, Chapter 6.
18. Venkataraman, K.; Choate, W. T.; Torre, E. R.; Husung, R. D.; Batchu, H. R. J Membr Sci 1998, 39, 259.
19. Hernández, A.; Calvo, J. I.; Prádanos, P.; Tejerina, F. J Membr Sci 1996, 112, 1.
20. Wortmann, F. J. Polymer 1996, 37, 2471.